Nonlinear Dyn manuscript No. (will be inserted by the editor) Trajectory design with finite time properties in precision positioning maneuvers

Efraín Ibarra
Instituto Tecnologico de Durango
Adrian Manzanilla
Centro de Investigacion y de Estudios Avanzados del IPN: Centro de Investigacion y de Estudios Avanzados del Instituto Politecnico Nacional
Pedro Castillo
Université de Technologie de Compiègne: Universite de Technologie de Compiegne
Ricardo Chapa (ricardo_rcg@hotmail.com)
Universidad Tecnológica Gral. Mariano Escobedo https://orcid.org/0000-0002-1676-9274

Research Article

Keywords: Finite time convergence, Open loop control, Robotic systems, Trajectory design

Posted Date: June 8th, 2022

DOI: https://doi.org/10.21203/rs.3.rs-1633961/v1

Nonlinear Dyn manuscript No.
(will be inserted by the editor)

Trajectory design with finite time properties in precision positioning maneuvers

Efraín Ibarra · Adrian Manzanilla · Pedro Castillo · Ricardo Chapa

Received: date / Accepted: date

Abstract In this paper is presented a new technique to design trajectories with finite time convergence properties for precision tracking maneuvers in unmanned vehicles. This technique allows the finite time positioning on sequentially distributed points, the properties for the trajectory guarantee to start in an initial point with velocity and acceleration zero, and position itself on the subsequent point with finite time convergence, again with velocity and acceleration zero. Such trajectory depends exclusively of the time and of the initial and last position. In addition, this technique could be used to design open loop controllers to be implemented in mobile robotics applications that require long accuracy. To show the controllers feasibility we considering the kinematic car model with finite time properties, obtaining an open loop control for the car's velocity and steering the vehicle to desired trajectory, where simulation results present the control performance and effectiveness.

Keywords Finite time convergence · Open loop control · Robotic systems · Trajectory design

E. Ibarra
Tecnológico Nacional de México
Instituto Tecnológico de Durango, C.P. 34080. México.
E-mail: efrainibarra@itdurango.edu.mx

A. Manzanilla
LAFMIA UMI - Cinvestav, Av Instituto Politécnico Nacional 2508,
San Pedro Zacatenco, 07360 Ciudad de México, CDMX.
E-mail: amanzanilla@cinvestav.mx

P. Castillo
Sorbonne Universités, Université de Technologie de Compiègne
CNRS, UMR 7253 Heudiasyc. France.
E-mail: pedro.castillo@hds.utc.fr

R. Chapa
Universidad Tecnológica Gral. Mariano Escobedo, Libramiento Noreste
Km 33.5 Gral. Escobedo, C.P 66050, Nuevo León.
E-mail: rgarcia@ute.edu.mx

1 Introduction

Navigation systems allow to guide in position and orientation a mobile robot from a starting point to a goal point in an indoor or outdoor environment. There are different proposals regarding the navigation of a mobile robot, most of them share a set of components, among which the location of the robot and generation of trajectories play a key role. In navigation systems, Global Positioning System (GPS) is used as position sensor, however, when GPS is not available, various methods are used to estimate the position of a vehicle. For example, in [2] presents complementary system navigation based on a method terrain aided navigation, which consists of estimating the speed of the vehicle referenced to the fixed body frame or the position to inertial frame using the existing digital terrain maps, that is, using exteropceptive sensors, terrain observations are obtained correlated with the known map a priori to calculate the pose of the robot. Instead, in [15] propose to estimate the position of a ground vehicle by data fusion through odometry and vision algorithm based on consensus-based tracking with a coincidence algorithm (CMT). Nevertheless, the most used technique to obtain the location of a vehicle is Dead Reckoning (DR) [6, 13, 14]; because a priori knowledge of the environment is not necessary. This technique is used when position sensors not yet available, and there are measurement sensors such as: encoder, IMU, AHRS, cameras, etc. The use of odometry by means of measurement sensors provides good precision in short periods and allows very high sampling rates; however, an accurate starting position quickly becomes uncertain through variations in vehicle movement, and position errors grow unlimitedly over time by accumulation of gyroscope and accelerometer error, as well as oscillatory speed errors that increase proportionally with the distance traveled by a mobile robot. Several works, have proposed the use of robust sensors

or the data fusion through Kalman filters to reduce accumulated errors. In [23], the authors present a method to correct navigation errors based on magnetic positioning to locate an automated guided vehicle (AGV), the magnetic sensor detects some properties of the magnetic field which are fused with the measurement of the sensors (encoder, IMU) to calculate and adjust the relative position of the AGV. Meanwhile in [3], is shown that through experimental results, the static and dynamic localization accuracy of the AGV can be improved using a laser positioning system and a matching algorithm based on Dead Reckoning. Other authors, propose use an AHRS and odometer to implement the Dead Reckoning technique, and for estimating the inclination of the orientation sensor, the authors add an extended Kalman filter (EKF) that helps to reduce the drift in the navigation system, obtaining a better precision even in the face of external disturbances, see [16].

Nowadays, there are proposals in the literature that only use crude measurements from an IMU to estimate the 3D pose of the vehicle using Dead Reckoning and implementing neural networks to adapt the covariance of an extended Kalman filter on the movements of the vehicle [1]. Other method to calibrate the model parameters, present in [19] propose a Dead reckoning calculation model through the fusion of complementary data and redundant sensors; furthermore, a Rauch-Tung-Striebel smoothing scheme is implemented to obtain smoothed estimates to calibrate the model parameters. Experimental tests demonstrate a system with reduced drift that provides a more accurate resulting model. In [4] a new traffic flow model called the forward-backward velocity difference (FBVD) model is presented, the model belongs to the family of microscopic models that consider spatiotemporally continuous formulations, through nonlinear analysis, a kink-antikink solution is derived from the modified Korteweg-de Vries equation to explain traffic congestion of the model. The dynamic performance of traffic flow using a modified optimal velocity car-following model was studied in [22], here a vehicle must adjust the following distance in real time, the results show that the proposed model improve the traffic stability and suppress traffic congestion. A new car-following (CF) model incorporating the effects of lateral gap and roadside device communication was proposed in [9], in this work the model stability is analyzed using perturbation method. An improved optimal velocity model, which considers the velocity difference of two adjacent lanes, is presented in [20], the nonlinear stability of the model is investigated and the solution of the modified Korteweg-de Vries equation near the critical points is obtained to characterize the unstable region. The process in the work [21] is to analyze the impacts of the green signal countdown device on car-following behaviors at signalized intersections and to propose an improved car-following model. The numerical results indicate that the improved car-following model can qualitatively describe the impacts of the green signal countdown device on car-following behaviors of the arrival traffic flow.

On the other hand, the trajectory generation presented by some authors, uses reference points, periodic orbits, geometric approaches, etc. For example, in [10, 18] the navigation method is presented by generating trajectory by waypoints to path planning future movements of the robot, the method in question, does not require prior knowledge of the environment and quickly generates adequate paths. However, there exist several ways to create dynamics, for instance, in [11] used periodic orbits in the form of regular polygons to carry out patrolling tasks in robots that drive in a straight line and use rebound angles.

The main contribution of this work is the development of a navigation technique where errors do not accumulate as time passes, thus, it is not necessary to adjust the drift. To introduce this technique we will take ideas from the papers [7, 8] where the authors propose a transient polynomial dynamic $\varphi(t)$ whose purpose is to prescribe to high-order sliding-modes in finite time and avoid the chartering effect into the designed controller capable to control the output of any smooth uncertain SISO system with known permanent relative degree [5, 12, 17]. The main idea is to modify the transient polynomial dynamics, which will be defined as $K_1(t)$ with the propose of designing a line $\mathbf{l}_{\mathrm{P_0P_1}}(t)$ that achieves the finite time positioning over a point $\mathbf{P}_1$ starting from $\mathbf{P}_0$, to continue, a second modified transient polynomial dynamic is introduced $K_2(t)$ to design a line $\mathbf{l}_{\mathrm{P_1P_2}}(t)$ that guarantees the finite time positioning over a point $\mathbf{P}_2$ starting from $\mathbf{P}_1$. Therefore, for $n+1$ points $\mathbf{P}_0, \mathbf{P}_1, \ldots, \mathbf{P}_n$ the general objective is to design recursively n modified transient polynomial dynamics $K_1(t)$, $K_2(t), \ldots, K_n(t)$ with the propose of designing n lines $\mathbf{l}_{\mathrm{P_0P_1}}(t)$, $\mathbf{l}_{\mathrm{P_1P_2}}(t)$, $\ldots$, $\mathbf{l}_{\mathrm{P_{n-1}P_n}}(t)$. Then, a switching technique will be introduced in order to do that each line $\mathbf{l}_{\mathrm{P_{i-1}P_i}}(t)$ occurs at its exact moment of appearance. Finally, a set of numerical simulations was performed to demonstrate the performance of the proposed method.

The remainder of the document is organized as follows: Section 2 describe the problem statement. Section 3 and 4, presents the main contributions of this paper, trajectory design with finite time convergence and trajectory with multiple finite time positioning. Then, Section 5 describe an educational example of consecutive trajectories by a simulation result. Section 6 provides a set of simulations to validate the open loop control of a ground vehicle using a trajectory with multiple finite time positioning, the main graphs illustrate the performance of the open-loop system. Finally, Section 7 presents a conclusions and future work.

2 Problem statement

In several applications using robots, it is necessary controllers that provides small errors for the mission. For some tasks the control accuracy is also related with the trajectory tracking, that in several cases is only given by a set of set points without any conditions in the robots.

For example, the line equation passing through two points $\mathbf{P}_0$ and $\mathbf{P}_1$ is represented in Fig. 1.

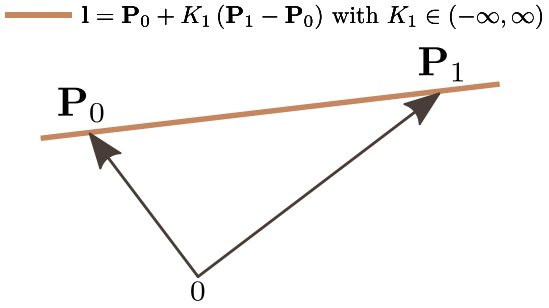

Fig. 1 Line representation between $\mathbf{P}_0$ and $\mathbf{P}_1$

where $\mathbf{l} \in \mathbb{R}^n$ with $n = 2, 3$.

Thus, several works use way points for a robot mission without imposing initial or final conditions for the robots that could degrade the robot's performances or damage it. In some cases, the previous can be solved tuning the control gains to improve the performance of the robot. Other solutions include the generation and tracking trajectory imposing some conditions in the robot for improving its behavior during the mission.

Our solution, presented in this paper, includes a new technique to design trajectories with multiple finite time positioning on sequential points $\mathbf{P}_0$, $\mathbf{P}_1$,..., $\mathbf{P}_n$ with the goal to use these trajectories in aerial or ground drones as path planning and as a manner to design open loop controllers to be implemented in precision agriculture missions.

Consequently, given $n+1$ points $\mathbf{P}_0$, $\mathbf{P}_1$, ..., $\mathbf{P}_n$ with $i = 1, \ldots, n$, we will design individual lines $\mathbf{l}_{\mathrm{P_{i-1}P_i}}(t)$ that pass through the points $\mathbf{P}_{i-1}$ and $\mathbf{P}_i$ where the finite time positioning on each one will be established, after that, a line $\mathbf{l}_r(t)$ will be the union of the previous lines, guaranteeing the following main properties.

2.1 Main properties

1. The convergence to the sequential points $\mathbf{P}_1$, $\mathbf{P}_2$, ..., $\mathbf{P}_n$ will be reached in finite time.
2. The time T_i in going from $\mathbf{P}_{i-1}$ to $\mathbf{P}_i$ will be established as we desire. However for our purposes this time will be proposed as $T_i = \mu \|\mathbf{P}_i - \mathbf{P}_{i-1}\|$ where μ is a proportionality constant and $\|\mathbf{P}_i - \mathbf{P}_{i-1}\|$ is the distance between the points $\mathbf{P}_{i-1}$ and $\mathbf{P}_i$.
3. We can propose a stop time ε over each sequential point, implying to stay on each point during a time ε before moving to the next point.
4. The velocity as well as the acceleration at the time $t_0 = 0$ seconds on $\mathbf{P}_0$ always are zero, and over the subsequent points $\mathbf{P}_1, \mathbf{P}_2, \ldots, \mathbf{P}_n$ the velocity and the acceleration will be maintained on zero during a lapse of time given by ε.

In fact, in real time experiments, where applications of high precision is required, the first and second property can guarantee finite time positioning on each point as well as to establish a finite time T_i in going from $\mathbf{P}_{i-1}$ to $\mathbf{P}_i$ although mathematically the finite time T_i can be chosen as small as we desire by the choice of a small parameter μ, it is important to clarify that in real time applications this time depends exclusively on the electronic and mechanical configuration of the motors of a robotic mobile vehicle. This means that for a mobile robotic application a minimal finite time $min(T_i)$ can be found by tuning the parameter μ, implying that $min(T_i) = min(\mu)\|\mathbf{P}_i - \mathbf{P}_{i-1}\|$ obtaining the fastest convergence at the point $\mathbf{P}_i$, then if we desired a smooth and slow finite time convergence T_i to go from $\mathbf{P}_{i-1}$ to $\mathbf{P}_i$ all the admissible parameters μ must satisfy $min(\mu) \leq \mu$. By another hand the third property guarantees the permanence on a point $\mathbf{P}_i$ during a lapse of time ε seconds, this means that a robot will remain static on $\mathbf{P}_i$ during a lapse of time ε, being able to perform some specific task.

3 Trajectory design with finite time convergence

3.1 Trajectory between two points

For some robot applications, trajectory tracking in fine time, with precision position control, is necessary for achieving the mission. Therefore, we are interested in designing a trajectory $\mathbf{l}_{\mathrm{P_0P_1}}(t)$ starting at time $t_0 = 0$ on the initial position $\mathbf{P}_0$ and steers until touching the point $\mathbf{P}_1$ in a desired finite time T_1. In addition, the trajectory must remain static on $\mathbf{P}_1$ during a stop time ε. In Fig. 2, the trajectory is graphically shown for 3D.

The trajectory $\mathbf{l}_{\mathrm{P_0P_1}}(t)$ and their derivatives $\dot{\mathbf{l}}_{\mathrm{P_0P_1}}(t)$, $\ddot{\mathbf{l}}_{\mathrm{P_0P_1}}(t)$ are described as

$$\mathbf{l}_{\mathrm{P_0P_1}}(t) = \mathbf{P}_0 + K_1(t)\Delta_{\mathbf{p_1}} \text{ with } K_1(t) \in [0,1] \tag{1a}$$

$$\dot{\mathbf{l}}_{\mathrm{P_0P_1}}(t) = \dot{K}_1(t)\Delta_{\mathbf{p_1}} \tag{1b}$$

$$\ddot{\mathbf{l}}_{\mathrm{P_0P_1}}(t) = \ddot{K}_1(t)\Delta_{\mathbf{p_1}} \tag{1c}$$

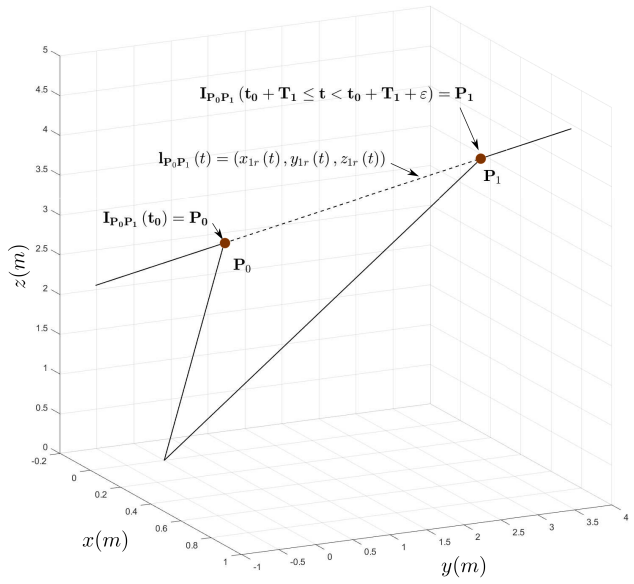

Fig. 2 Trajectory $\mathbf{l}_{\mathrm{P_0P_1}}(t)$ with points $\mathbf{P}_0, \mathbf{P}_1 \in \mathbb{R}^3$

where $\Delta_{\mathbf{p_1}} = \mathbf{P}_1 - \mathbf{P}_0$ and $K_1(t)$, $\dot{K}_1(t)$, $\ddot{K}_1(t)$ are time functions given by

$$K_1(t) = \begin{cases} 1 + (t-(t_0+T_1))^3 \psi_1(t) & t \in [t_0, t_0+T_1) \\ 1 & t \in [t_0+T_1, t_0+T_1+\varepsilon) \end{cases}$$

$$\dot{K}_1(t) = \begin{cases} 3(t-(t_0+T_1))^2 \psi_1(t) \\ +(t-(t_0+T_1))^3 \dot{\psi}_1(t) & t \in [t_0, t_0+T_1) \\ 0 & t \in [t_0+T_1, t_0+T_1+\varepsilon) \end{cases}$$

$$\ddot{K}_1(t) = \begin{cases} 6(t-(t_0+T_1))\psi_1(t) \\ +6(t-(t_0+T_1))^2 \dot{\psi}_1 \\ +(t-(t_0+T_1))^3 \ddot{\psi}_1(t) & t \in [t_0, t_0+T_1) \\ 0 & t \in [t_0+T_1, t_0+T_1+\varepsilon) \end{cases}$$

where T_1 is the time in going from $\mathbf{P}_0$ to $\mathbf{P}_1$, the scalar ε is the stop time on $\mathbf{P}_1$ and ψ_1, $\dot{\psi}_1$, $\ddot{\psi}_1$ are represented as

$$\begin{aligned} \psi_1(t) &= \mathrm{a}_1 + \mathrm{b}_1(t-t_0) + \mathrm{c}_1(t-t_0)^2, \\ \dot{\psi}_1(t) &= \mathrm{b}_1 + 2\mathrm{c}_1(t-t_0), \\ \ddot{\psi}_1(t) &= 2\mathrm{c}_1, \end{aligned}$$

with $t_0 = 0$, as the initial time.

and the coefficients $\mathrm{a}_1, \mathrm{b}_1, \mathrm{c}_1$ must be selected in order to fulfill the following lemma.

Lemma 1 *Define* a_1, b_1, c_1 *in* $K_1(t)$, $\dot{K}_1(t)$, $\ddot{K}_1(t)$ *as*

$$\mathrm{a}_1 = \frac{1}{T_1^3}; \quad \mathrm{b}_1 = \frac{3\mathrm{a}_1}{T_1}; \quad \mathrm{c}_1 = \frac{3(\mathrm{b}_1 T_1 - \mathrm{a}_1)}{T_1^2} \tag{2}$$

then, the following properties are satisfied

Property 1*:* $K_1(t_0) = 0$*;* $K_1(t_1) = 1$.

Property 2*:* $\dot{K}_1(t_0) = 0$*:* $\dot{K}_1(t_1) = 0$.

Property 3*:* $\ddot{K}_1(t_0) = 0$*;* $\ddot{K}_1(t_1) = 0$.

with $t_1 = t_0 + T_1 \leq t < t_0 + T_1 + \varepsilon$*; guarantying that*

$$\mathbf{l}_{\mathrm{P_0P_1}}(t_0) = \mathbf{P}_0; \qquad \mathbf{l}_{\mathrm{P_0P_1}}(t_1) = \mathbf{P}_1 \tag{3a}$$

$$\dot{\mathbf{l}}_{\mathrm{P_0P_1}}(t_0) = \mathbf{0}; \qquad \dot{\mathbf{l}}_{\mathrm{P_0P_1}}(t_1) = \mathbf{0} \tag{3b}$$

$$\ddot{\mathbf{l}}_{\mathrm{P_0P_1}}(t_0) = \mathbf{0}; \qquad \ddot{\mathbf{l}}_{\mathrm{P_0P_1}}(t_1) = \mathbf{0} \tag{3c}$$

Proof The proof consists in choosing T_1 and computes firstly the value of a_1, secondly b_1, and at the end c_1 as in (2). At the end, observe that the above three properties are satisfied, implying that (3a), (3b) and (3c) are true.■

Example: trajectory in 2D

Let consider $\mathbf{P}_0$, $\mathbf{P}_1 \in \mathbb{R}^2$ where $\mathbf{P}_0 = (x_0, y_0)$, $\mathbf{P}_1 = (x_{d_1}, y_{d_1})$ and define $\mathbf{l}_{\mathrm{P_0P_1}}(t) = (x_{1r}(t), y_{1r}(t))$. Therefore, (1a), (1b) and (1c) can be represented as

$$(x_{1r}(t), y_{1r}(t)) = (x_0, y_0) + K_1(t)\left(x_{d_1} - x_0, y_{d_1} - y_0\right); \tag{4a}$$

$$(\dot{x}_{1r}(t), \dot{y}_{1r}(t)) = \dot{K}_1(t)\left(x_{d_1} - x_0, y_{d_1} - y_0\right); \tag{4b}$$

$$(\ddot{x}_{1r}(t), \ddot{y}_{1r}(t)) = \ddot{K}_1(t)\left(x_{d_1} - x_0, y_{d_1} - y_0\right); \tag{4c}$$

or by components

$$\begin{aligned} x_{1r}(t) &= x_0 + K_1(t)(x_{d_1} - x_0); \\ y_{1r}(t) &= y_0 + K_1(t)(y_{d_1} - y_0); \end{aligned} \tag{5a}$$

$$\begin{aligned} \dot{x}_{1r}(t) &= \dot{K}_1(t)(x_{d_1} - x_0); \\ \dot{y}_{1r}(t) &= \dot{K}_1(t)(y_{d_1} - y_0); \end{aligned} \tag{5b}$$

$$\begin{aligned} \ddot{x}_{1r}(t) &= \ddot{K}_1(t)(x_{d_1} - x_0); \\ \ddot{y}_{1r}(t) &= \ddot{K}_1(t)(y_{d_1} - y_0); \end{aligned} \tag{5c}$$

Similarly, the expressions (3a), (3b) and (3c) become

$$\begin{aligned} x_{1r}(t_0) &= x_0; & x_{1r}(t_1) &= x_{d_1} \\ y_{1r}(t_0) &= y_0; & y_{1r}(t_1) &= y_{d_1} \end{aligned} \tag{6a}$$

$$\begin{aligned} \dot{x}_{1r}(t_0) &= 0; & \dot{x}_{1r}(t_1) &= 0 \\ \dot{y}_{1r}(t_0) &= 0; & \dot{y}_{1r}(t_1) &= 0 \end{aligned} \tag{6b}$$

$$\begin{aligned} \ddot{x}_{1r}(t_0) &= 0; & \ddot{x}_{1r}(t_1) &= 0 \\ \ddot{y}_{1r}(t_0) &= 0; & \ddot{y}_{1r}(t_1) &= 0 \end{aligned} \tag{6c}$$

3.2 Trajectory in three set-points

Let define ε as a bounded scalar, therefore a second trajectory, $\mathbf{l}_{\mathrm{P_1P_2}}(t)$, can be introduced starting at time $T_1 + \varepsilon$ on the point $\mathbf{P}_1$ and steers until touching a third point $\mathbf{P}_2$ in a desired finite time $T_1 + \varepsilon + T_2$, where T_2 is the necessary time to go from $\mathbf{P_1}$ to $\mathbf{P_2}$.

Rewriting the trajectory $\mathbf{l}_{\mathrm{P_1P_2}}(t)$ and their derivatives $\dot{\mathbf{l}}_{\mathrm{P_1P_2}}(t)$, $\ddot{\mathbf{l}}_{\mathrm{P_1P_2}}(t)$ as in (1a)–(1c), it follows that

$$\mathbf{l}_{\mathrm{P_1P_2}}(t) = \mathbf{P}_1 + K_2(t)\,\Delta_{\mathbf{p}_2} \text{ with } K_2(t) \in [0,1] \tag{7a}$$
$$\dot{\mathbf{l}}_{\mathrm{P_1P_2}}(t) = \dot{K}_2(t)\Delta_{\mathbf{p}_2} \tag{7b}$$
$$\ddot{\mathbf{l}}_{\mathrm{P_1P_2}}(t) = \ddot{K}_2(t)\Delta_{\mathbf{p}_2} \tag{7c}$$

with $\Delta_{\mathbf{p}_2} = (\mathbf{P}_2 - \mathbf{P}_1)$ and $K_2(t)$, $\dot{K}_2(t)$, $\ddot{K}_2(t)$ are defined as

$$K_2(t) = \begin{cases} 1 + (t-(t_{f_1}+T_2))^3\psi_2(t) & t \in \left[t_{f_1}, t_{f_1}+T_2\right) \\ 1 & t \in \left[t_{f_1}+T_2, t_{f_1}+T_2+\varepsilon\right) \end{cases}$$

$$\dot{K}_2(t) = \begin{cases} 3(t-(t_{f_1}+T_2))^2\psi_2(t) \\ +(t-(t_{f_1}+T_2))^3\dot{\psi}_2(t) & t \in [t_{f_1}, t_{f_1}+T_2) \\ 0 & t \in \left[t_{f_1}+T_2, t_{f_1}+T_2+\varepsilon\right) \end{cases}$$

$$\ddot{K}_2(t) = \begin{cases} 6(t-(t_{f_1}+T_2))\psi_2(t) \\ +6(t-(t_{f_1}+T_2))^2\dot{\psi}_2(t) \\ +(t-(t_{f_1}+T_2))^3\ddot{\psi}_2(t) & t \in [t_{f_1}, t_{f_1}+T_2) \\ 0 & t \in \left[t_{f_1}+T_2, t_{f_1}+T_2+\varepsilon\right) \end{cases}$$

where T_2 is the time in going from $\mathbf{P}_1$ to $\mathbf{P}_2$, and ε is the stop time on $\mathbf{P}_2$ and ψ_2, $\dot{\psi}_2$, $\ddot{\psi}_2$ are represented as

$$\begin{aligned} \psi_2(t) &= \mathrm{a}_2 + \mathrm{b}_2(t-t_{f_1}) + \mathrm{c}_2(t-t_{f_1})^2, \\ \dot{\psi}_2(t) &= \mathrm{b}_2 + 2\mathrm{c}_2(t-t_{f_1}), \\ \ddot{\psi}_2(t) &= 2\mathrm{c}_2, \\ \text{with } t_{f_1} &= T_1 + \varepsilon. \end{aligned}$$

In addition, Lemma 1 can be rewritten for a_2, b_2, c_2 as

$$\mathrm{a}_2 = \frac{1}{T_2^3}; \quad \mathrm{b}_2 = \frac{3\mathrm{a}_2}{T_2}; \quad \mathrm{c}_2 = \frac{3(\mathrm{b}_2 T_2 - \mathrm{a}_2)}{T_2^2} \tag{8}$$

and the three properties can be obtained as

(**Prop 1**). $K_2(t_{f_1}) = 0$; $K_2(t_2) = 1$.
(**Prop 2**). $\dot{K}_2(t_{f_1}) = 0$; $\dot{K}_2(t_2) = 0$.
(**Prop 3**). $\ddot{K}_2(t_{f_1}) = 0$; $\ddot{K}_2(t_2) = 0$.

with $t_2 = t_{f_1} + T_2 \leq t < t_{f_1} + T_2 + \varepsilon$.

The above properties guarantee that

$$\mathbf{l}_{\mathrm{P_1P_2}}(t_{f_1}) = \mathbf{P}_1 \text{ and } \mathbf{l}_{\mathrm{P_1P_2}}(t_2) = \mathbf{P}_2 \tag{9a}$$
$$\dot{\mathbf{l}}_{\mathrm{P_1P_2}}(t_{f_1}) = \mathbf{0} \text{ and } \dot{\mathbf{l}}_{\mathrm{P_1P_2}}(t_2) = \mathbf{0} \tag{9b}$$
$$\ddot{\mathbf{l}}_{\mathrm{P_1P_2}}(t_{f_1}) = \mathbf{0} \text{ and } \ddot{\mathbf{l}}_{\mathrm{P_1P_2}}(t_2) = \mathbf{0} \tag{9c}$$

Example: trajectory in 2D

Let consider $\mathbf{P}_2 = (x_{d_2}, y_{d_2})$ and $\mathbf{l}_{\mathrm{P_1P_2}}(t) = (x_{1r}(t), y_{1r}(t))$ validated from t_{f_1} to $t_{f_1} + T_2 + \varepsilon$, then (7a)–(7c) can be rewritten as

$$(x_{1r}(t), y_{1r}(t)) = (x_{d_1}, y_{d_1}) + K_2(t)\left(x_{d_2} - x_{d_1}, y_{d_2} - y_{d_1}\right) \tag{10a}$$
$$(\dot{x}_{1r}(t), \dot{y}_{1r}(t)) = \dot{K}_2(t)\left(x_{d_2} - x_{d_1}, y_{d_2} - y_{d_1}\right) \tag{10b}$$
$$(\ddot{x}_{1r}(t), \ddot{y}_{1r}(t)) = \ddot{K}_2(t)\left(x_{d_2} - x_{d_1}, y_{d_2} - y_{d_1}\right) \tag{10c}$$

with

$$\begin{aligned} x_{1r}(t_{f_1}) &= x_{d_1}; & x_{1r}(t_2) &= x_{d_2} \\ y_{1r}(t_{f_1}) &= y_{d_1}; & y_{1r}(t_2) &= y_{d_2} \end{aligned} \tag{11a}$$

$$\begin{aligned} \dot{x}_{1r}(t_{f_1}) &= 0; & \dot{x}_{1r}(t_2) &= 0 \\ \dot{y}_{1r}(t_{f_1}) &= 0; & \dot{y}_{1r}(t_2) &= 0 \end{aligned} \tag{11b}$$

$$\begin{aligned} \ddot{x}_{1r}(t_{f_1}) &= 0; & \ddot{x}_{1r}(t_2) &= 0 \\ \ddot{y}_{1r}(t_{f_1}) &= 0; & \ddot{y}_{1r}(t_2) &= 0 \end{aligned} \tag{11c}$$

3.3 Trajectory with $n+1$ set-points

Let consider $n+1$ points; $\mathbf{P}_0$, $\mathbf{P}_1$, $\mathbf{P}_2$, …, $\mathbf{P}_{n-1}$, $\mathbf{P}_n$, therefore, it is possible to design n lines given by $\mathbf{l}_{\mathrm{P_0P_1}}(t)$, $\mathbf{l}_{\mathrm{P_1P_2}}(t)$, … , $\mathbf{l}_{\mathrm{P_{n-1}P_n}}(t)$, where each one is validated into their respective interval of time. Table 1 summarizes the interval of time for each trajectory $\mathbf{l}_{\mathrm{P_{i-1}P_i}}(t)$ with $i = 1, 2, 3, \ldots, n$.

Table 1 Interval of time, terminal time t_{f_i} and convergence time T_i parameters in each trajectory.

$\mathbf{l}_{\mathrm{P}_{i-1}\mathrm{P}_i}(t)$	Interval of time	Terminal time t_{f_i}	$T_i = \mu\,\lVert\mathbf{P}_i - \mathbf{P}_{i-1}\rVert$
$\mathbf{l}_{\mathrm{P_0P_1}}(t)$	$0 \leq t < t_{f_1}$	$t_{f_1} = T_1 + \varepsilon$	$T_1 = \mu\,\lVert\mathbf{P}_1 - \mathbf{P}_0\rVert$
$\mathbf{l}_{\mathrm{P_1P_2}}(t)$	$t_{f_1} \leq t < t_{f_2}$	$t_{f_2} = t_{f_1} + T_2 + \varepsilon$	$T_2 = \mu\,\lVert\mathbf{P}_2 - \mathbf{P}_1\rVert$
$\mathbf{l}_{\mathrm{P_2P_3}}(t)$	$t_{f_2} \leq t < t_{f_3}$	$t_{f_3} = t_{f_2} + T_3 + \varepsilon$	$T_3 = \mu\,\lVert\mathbf{P}_3 - \mathbf{P}_2\rVert$
$\mathbf{l}_{\mathrm{P_3P_4}}(t)$	$t_{f_3} \leq t < t_{f_4}$	$t_{f_4} = t_{f_3} + T_4 + \varepsilon$	$T_4 = \mu\,\lVert\mathbf{P}_4 - \mathbf{P}_3\rVert$
⋮	⋮	⋮	⋮
$\mathbf{l}_{\mathrm{P_{n-1}P_n}}(t)$	$t_{f_{n-1}} \leq t < t_{f_n}$	$t_{f_n} = t_{f_{n-1}} + T_n + \varepsilon$	$T_n = \mu\,\lVert\mathbf{P}_n - \mathbf{P}_{n-1}\rVert$

For describing the general trajectory, the following definitions are necessary.

Definition 1 (Interval of time) This interval of time corresponds at the time where the line $\mathbf{l}_{\mathrm{P}_{i-1}\mathrm{P}_i}(t)$ is validated.

Definition 2 (Terminal time t_{f_i}) It is the last time where the line $\mathbf{l}_{\mathrm{P}_{i-1}\mathrm{P}_i}(t)$ is validated, and is calculated as $t_{f_i} = \sum_{j=1}^{i} T_j + i \times \varepsilon$.

Definition 3 (Stop time ε) The lapse of time when the line $\mathbf{l}_{\mathrm{P}_{i-1}\mathrm{P}_i}(t)$ remains motionless on the point $\mathbf{P}_i$.

Definition 4 (Convergence time T_i) T_i is defined as the necessary time to go from $\mathbf{P}_{i-1}$ to $\mathbf{P}_i$. It can be proposed by the user as desired. Nevertheless, for robot applications, a convenient manner is to suppose that T_i is directly proportional to the distance between $\mathbf{P}_{i-1}$ and $\mathbf{P}_i$. Therefore, it can computed as $T_i = \mu \|\mathbf{P}_i - \mathbf{P}_{i-1}\|$, where μ is a proportionality constant, see right column in Table 1.

Note that the following algorithm is valid if at least two points $\mathbf{P}_0$ and $\mathbf{P}_1$ are defined. Therefore, for the trajectories $i = 1,2,3,\ldots,n$, each line $\mathbf{l}_{\mathrm{P_{i-1}P_i}}(t)$ and their derivatives $\dot{\mathbf{l}}_{\mathrm{P_{i-1}P_i}}(t)$, $\ddot{\mathbf{l}}_{\mathrm{P_{i-1}P_i}}(t)$ can be denoted as

$$\mathbf{l}_{\mathrm{P_{i-1}P_i}}(t) = \mathbf{P}_{i-1} + K_i(t)\,\Delta_{\mathbf{p}_i} \text{ with } K_i(t) \in [0,1] \tag{12a}$$
$$\dot{\mathbf{l}}_{\mathrm{P_{i-1}P_i}}(t) = \dot{K}_i(t)\Delta_{\mathbf{p}_i} \tag{12b}$$
$$\ddot{\mathbf{l}}_{\mathrm{P_{i-1}P_i}}(t) = \ddot{K}_i(t)\Delta_{\mathbf{p}_i} \tag{12c}$$

with $\Delta_{\mathbf{p}_i} = (\mathbf{P}_i - \mathbf{P}_{i-1})$ and

$$K_i(t) = \begin{cases} 1 + (t - (t_{f_{i-1}} + T_i))^3 \psi_i(t) & t \in \left[t_{f_{i-1}}, t_{f_{i-1}} + T_i\right) \\ 1 & t \in \left[t_{f_{i-1}} + T_i, t_{f_{i-1}} + T_i + \varepsilon\right) \end{cases}$$

$$\dot{K}_i(t) = \begin{cases} 3(t - (t_{f_{i-1}} + T_i))^2 \psi_i(t) & \\ +(t - (t_{f_{i-1}} + T_i))^3 \dot{\psi}_i(t) & t \in [t_{f_{i-1}}, t_{f_{i-1}} + T_i) \\ 0 & t \in \left[t_{f_{i-1}} + T_i, t_{f_{i-1}} + T_i + \varepsilon\right) \end{cases}$$

$$\ddot{K}_i(t) = \begin{cases} 6(t - (t_{f_{i-1}} + T_i))\psi_i(t) & \\ +6(t - (t_{f_{i-1}} + T_i))^2 \dot{\psi}_i(t) & t \in [t_{f_{i-1}}, t_{f_{i-1}} + T_i) \\ +(t - (t_{f_{i-1}} + T_i))^3 \ddot{\psi}_i(t) & \\ 0 & t \in \left[t_{f_{i-1}} + T_i, t_{f_{i-1}} + T_i + \varepsilon\right) \end{cases}$$

where T_i is the time in going from $\mathbf{P}_{i-1}$ to $\mathbf{P}_i$, and ε is the stop time on $\mathbf{P}_i$ and ψ_i, $\dot{\psi}_i$, $\ddot{\psi}_i$ are represented as

$$\begin{aligned} \psi_i(t) &= \mathrm{a}_i + \mathrm{b}_i(t - t_{f_{i-1}}) + \mathrm{c}_i(t - t_{f_{i-1}})^2, \\ \dot{\psi}_i(t) &= \mathrm{b}_i + 2\mathrm{c}_i(t - t_{f_{i-1}}), \\ \ddot{\psi}_i(t) &= 2\mathrm{c}_i \end{aligned}$$

$$t_{f_{i-1}} = \sum_{j=1}^{i-1} T_j + (i-1)\times\varepsilon, \text{ validated from } i = 2 \text{ to } n.$$

only for the case $i = 1$, we will have $t_{f_0} = t_0 = 0$. In addition, if the coefficients a_i, b_i, c_i are selected as

$$\mathrm{a}_i = \frac{1}{T_i^3}; \quad \mathrm{b}_i = \frac{3\mathrm{a}_i}{T_i}; \quad \mathrm{c}_i = \frac{3(\mathrm{b}_i T_i - \mathrm{a}_i)}{T_i^2} \tag{13}$$

then the following properties are guaranteed

(**a**).- $K_i(t_{f_{i-1}}) = 0 \qquad K_i(t_i) = 1.$
(**b**).- $\dot{K}_i(t_{f_{i-1}}) = 0 \qquad \dot{K}_i(t_i) = 0.$
(**c**).- $\ddot{K}_i(t_{f_{i-1}}) = 0 \qquad \ddot{K}_i(t_i) = 0.$

with $t_i = t_{f_{i-1}} + T_i \le t < t_{f_{i-1}} + T_i + \varepsilon$. The above implies that

$$\mathbf{l}_{\mathrm{P_{i-1}P_i}}(t_{f_{i-1}}) = \mathbf{P}_{i-1} \qquad \mathbf{l}_{\mathrm{P_{i-1}P_i}}(t_i) = \mathbf{P}_i \tag{14a}$$
$$\dot{\mathbf{l}}_{\mathrm{P_{i-1}P_i}}(t_{f_{i-1}}) = \mathbf{0} \qquad \dot{\mathbf{l}}_{\mathrm{P_{i-1}P_i}}(t_i) = \mathbf{0} \tag{14b}$$
$$\ddot{\mathbf{l}}_{\mathrm{P_{i-1}P_i}}(t_{f_{i-1}}) = \mathbf{0} \qquad \ddot{\mathbf{l}}_{\mathrm{P_{i-1}P_i}}(t_i) = \mathbf{0} \tag{14c}$$

Similarly, $\mathbf{l}_{\mathrm{P_{i-1}P_i}}(t) = (x_{1r}(t), y_{1r}(t))$, validated only for the time interval $t_{f_{i-1}} \le t < t_{f_i}$, can be also represented as

$$\begin{aligned} (x_{1r}(t), y_{1r}(t)) &= (x_{d_{i-1}}, y_{d_{i-1}}) + K_i(t)\left(x_{d_i} - x_{d_{i-1}}, y_{d_i} - y_{d_{i-1}}\right) \\ (\dot{x}_{1r}(t), \dot{y}_{1r}(t)) &= \dot{K}_i(t)\left(x_{d_i} - x_{d_{i-1}}, y_{d_i} - y_{d_{i-1}}\right) \\ (\ddot{x}_{1r}(t), \ddot{y}_{1r}(t)) &= \ddot{K}_i(t)\left(x_{d_i} - x_{d_{i-1}}, y_{d_i} - y_{d_{i-1}}\right) \end{aligned}$$

or defined in the components of position, velocity and acceleration are described as

$$\begin{aligned} x_{1r}(t) &= x_{d_{i-1}} + K_i(t)(x_{d_i} - x_{d_{i-1}}) \\ y_{1r}(t) &= y_{d_{i-1}} + K_i(t)(y_{d_i} - y_{d_{i-1}}) \end{aligned} \tag{15a}$$
$$\begin{aligned} \dot{x}_{1r}(t) &= \dot{K}_i(t)(x_{d_i} - x_{d_{i-1}}) \\ \dot{y}_{1r}(t) &= \dot{K}_i(t)(y_{d_i} - y_{d_{i-1}}) \end{aligned} \tag{15b}$$
$$\begin{aligned} \ddot{x}_{1r}(t) &= \ddot{K}_i(t)(x_{d_i} - x_{d_{i-1}}) \\ \ddot{y}_{1r}(t) &= \ddot{K}_i(t)(y_{d_i} - y_{d_{i-1}}) \end{aligned} \tag{15c}$$

Remark 1 Observe that $K_i(t)$, $\dot{K}_i(t)$, $\ddot{K}_i(t)$ satisfy the properties (**a**), (**b**) and (**c**) respectively, these variables can be seen as control variables with temporal dependency.

For example, $K_i(t)$ is the **open loop control position**, accomplishing that (15a) satisfies (14a). Similarly, $\dot{K}_i(t)$ is the **open loop control velocity**, making (15b) satisfies (14b). In addition, $\ddot{K}_i(t)$ is the **open loop control acceleration**, doing (15c) satisfies (14c).

4 General trajectory with multiple finite time position

Each sequential trajectory $\mathbf{l}_{\mathrm{P_{i-1}P_i}}(t)$, composes a general trajectory $\mathbf{l}_r(t)$ validated from $t_0 = 0$ to t_{f_n} and defined as

$$\begin{aligned} \mathbf{l}_r(t) = {} & g_1(t)\mathbf{l}_{\mathrm{P_0P_1}}(t) + f_1(t)g_2(t)\mathbf{l}_{\mathrm{P_1P_2}}(t) + f_2(t)g_3(t)\mathbf{l}_{\mathrm{P_2P_3}}(t) \\ & + \ldots + f_{n-1}(t)g_n(t)\mathbf{l}_{\mathrm{P_{n-1}P_n}}(t) \end{aligned}$$

or

$$\mathbf{l}_r(t) = g_1(t)\mathbf{l}_{\mathrm{P_0P_1}}(t) + \sum_{i=2}^{n} f_{i-1}(t)g_i(t)\mathbf{l}_{\mathrm{P_{i-1}P_i}}(t) \tag{16}$$

where $g_1(t)$, $g_2(t)$, $g_3(t)$, ... , $g_{n-1}(t)$, $g_n(t)$ and $f_1(t)$, $f_2(t)$, $f_3(t)$, ... , $f_{n-1}(t)$ are given as

$$g_1(t)=\begin{cases}1 \text{ for } 0\le t<t_{f_1}\\ 0 \text{ for } t_{f_1}\le t\end{cases}\quad f_1(t)=\begin{cases}0 \text{ for } 0\le t<t_{f_1}\\ 1 \text{ for } t_{f_1}\le t\end{cases}$$
$$g_2(t)=\begin{cases}1 \text{ for } 0\le t<t_{f_2}\\ 0 \text{ for } t_{f_2}\le t\end{cases}\quad f_2(t)=\begin{cases}0 \text{ for } 0\le t<t_{f_2}\\ 1 \text{ for } t_{f_2}\le t\end{cases}$$
$$g_3(t)=\begin{cases}1 \text{ for } 0\le t<t_{f_3}\\ 0 \text{ for } t_{f_3}\le t\end{cases}\quad f_3(t)=\begin{cases}0 \text{ for } 0\le t<t_{f_3}\\ 1 \text{ for } t_{f_3}\le t\end{cases}$$
$$\vdots \qquad\qquad \vdots$$
$$g_{n-1}(t)=\begin{cases}1 \text{ for } 0\le t<t_{f_{n-1}}\\ 0 \text{ for } t_{f_{n-1}}\le t\end{cases}\quad f_{n-1}(t)=\begin{cases}0 \text{ for } 0\le t<t_{f_{n-1}}\\ 1 \text{ for } t_{f_{n-1}}\le t\end{cases}$$
$$g_n(t)=\begin{cases}1 \text{ for } 0\le t<t_{f_n}\\ 0 \text{ for } \quad t_{f_n}\le t\end{cases}$$

From Table 1, it follows that $t_{f_1}<t_{f_2}<t_{f_3}<\ldots<t_{f_{n-1}}<t_{f_n}$, implying that $f_1(t)g_2(t)$, $f_2(t)g_3(t)$, ... ,$f_{n-1}(t)g_n(t)$ are given as

$$f_1(t)g_2(t)=\begin{cases}0 \text{ for } 0\le t<t_{f_1}\\ 1 \text{ for } t_{f_1}\le t<t_{f_2}\\ 0 \text{ for } t_{f_2}\le t\end{cases}$$
$$f_2(t)g_3(t)=\begin{cases}0 \text{ for } 0\le t<t_{f_2}\\ 1 \text{ for } t_{f_2}\le t<t_{f_3}\\ 0 \text{ for } t_{f_3}\le t\end{cases}$$
$$\vdots$$
$$f_{n-1}(t)g_n(t)=\begin{cases}0 \text{ for } 0\le t<t_{f_{n-1}}\\ 1 \text{ for } t_{f_{n-1}}\le t<t_{f_n}\\ 0 \text{ for } t_{f_n}\le t.\end{cases}$$

Observe that $g_1(t)$, $f_1(t)g_2(t)$, $f_2(t)g_3(t)$,..., $f_{n-1}(t)g_n(t)$ activate the trajectories $\mathbf{l}_{\mathrm{P_{i-1}P_i}}(t)$ in their respective time-interval $t_{f_{i-1}}\le t<t_{f_i}$, i.e.,

$$\begin{aligned}&\mathbf{l}_r(t)=\mathbf{l}_{\mathrm{P_0P_1}}(t) \quad for \quad 0\le t<t_{f_1}\\ &\mathbf{l}_r(t)=\mathbf{l}_{\mathrm{P_1P_2}}(t) \quad for \quad t_{f_1}\le t<t_{f_2}\\ &\mathbf{l}_r(t)=\mathbf{l}_{\mathrm{P_2P_3}}(t) \quad for \quad t_{f_2}\le t<t_{f_3}\\ &\qquad\vdots\\ &\mathbf{l}_r(t)=\mathbf{l}_{\mathrm{P_{n-1}P_n}}(t) \; for \; t_{f_{n-1}}\le t<t_{f_n}\end{aligned}$$

Therefore we are obligated to introduce the following definition.

Definition 5 . The time functions $g_1(t)$, $f_1(t)g_2(t)$, $f_2(t)g_3(t)$, ..., $f_{n-1}(t)g_n(t)$ responsible to activate the trajectories $\mathbf{l}_{\mathrm{P_{i-1}P_i}}(t)$ in their respective time-interval $t_{f_{i-1}}\le t<t_{f_i}$ will be named the "*temporal activation functions*".

From (16), it follows that

$$\dot{\mathbf{l}}_r(t)=g_1(t)\dot{\mathbf{l}}_{\mathrm{P_0P_1}}(t)+\sum_{i=2}^{n}f_{i-1}(t)g_i(t)\dot{\mathbf{l}}_{\mathrm{P_{i-1}P_i}}(t) \tag{17a}$$
$$\ddot{\mathbf{l}}_r(t)=g_1(t)\ddot{\mathbf{l}}_{\mathrm{P_0P_1}}(t)+\sum_{i=2}^{n}f_{i-1}(t)g_i(t)\ddot{\mathbf{l}}_{\mathrm{P_{i-1}P_i}}(t) \tag{17b}$$

Defining $\mathbf{l}_r(t)=(x_{1r}(t),y_{1r}(t))$, $\dot{\mathbf{l}}_r(t)=(\dot{x}_{1r}(t),\dot{y}_{1r}(t))$ and $\ddot{\mathbf{l}}_r(t)=(\ddot{x}_{1r}(t),\ddot{y}_{1r}(t))$ and considering (16), (17a) and (17b), it follows that

$$\begin{aligned}x_{1r}(t)=&(x_0+K_1(t)(x_{d_1}-x_0))g_1(t)\\ &+\sum_{i=2}^{n}f_{i-1}(t)g_i(t)(x_{d_{i-1}}+K_i(t)(x_{d_i}-x_{d_{i-1}}))\end{aligned} \tag{18a}$$
$$\begin{aligned}y_{1r}(t)=&(y_0+K_1(t)(y_{d_1}-y_0))g_1(t)\\ &+\sum_{i=2}^{n}f_{i-1}(t)g_i(t)(y_{d_{i-1}}+K_i(t)(y_{d_i}-y_{d_{i-1}}))\end{aligned} \tag{18b}$$
$$\begin{aligned}\dot{x}_{1r}(t)=&\dot{K}_1(t)(x_{d_1}-x_0)g_1(t)+\\ &+\sum_{i=2}^{n}f_{i-1}(t)g_i(t)\dot{K}_i(t)(x_{d_i}-x_{d_{i-1}})\end{aligned} \tag{18c}$$
$$\begin{aligned}\dot{y}_{1r}(t)=&\dot{K}_1(t)(y_{d_1}-y_0)g_1(t)\\ &+\sum_{i=2}^{n}f_{i-1}(t)g_i(t)\dot{K}_i(t)(y_{d_i}-y_{d_{i-1}})\end{aligned} \tag{18d}$$
$$\begin{aligned}\ddot{x}_{1r}(t)=&\ddot{K}_1(t)(x_{d_1}-x_0)g_1(t)\\ &+\sum_{i=2}^{n}f_{i-1}(t)g_i(t)\ddot{K}_i(t)(x_{d_i}-x_{d_{i-1}})\end{aligned} \tag{18e}$$
$$\begin{aligned}\ddot{y}_{1r}(t)=&\ddot{K}_1(t)(y_{d_1}-y_0)g_1(t)\\ &+\sum_{i=2}^{n}f_{i-1}(t)g_i(t)\ddot{K}_i(t)(y_{d_i}-y_{d_{i-1}})\end{aligned} \tag{18f}$$

4.1 Example: 2D Trajectory with five points

Let consider a trajectory composed by five points defined as $\mathbf{P}_0=(x_0,y_0)=(1,1)$; $\mathbf{P}_1=(x_{d_1},y_{d_1})=(2,2.5)$; $\mathbf{P}_2=(x_{d_2},y_{d_2})=(4.5,1.2)$; $\mathbf{P}_3=(x_{d_3},y_{d_3})=(5.5,2)$; and $\mathbf{P}_4=(x_{d_4},y_{d_4})=(6,3.5)$ in meters. $\mathbf{P}_0$ defines the initial position.

To obtain the trajectory $\mathbf{l}_r(t)$, the first step is to design the four consecutive trajectories $\mathbf{l}_{\mathrm{P_0P_1}}(t)$, $\mathbf{l}_{\mathrm{P_1P_2}}(t)$, $\mathbf{l}_{\mathrm{P_2P_3}}(t)$, $\mathbf{l}_{\mathrm{P_3P_4}}(t)$ validated into the respective time interval $t_{f_{i-1}}\le t<t_{f_i}$ for $i=1,2,3,4$. Moreover, from Table 1, and proposing a proportionality constant $\mu=1.5$, T_i can be computed as

$$\begin{aligned}T_1&=\mu\,\|\mathbf{P}_1-\mathbf{P}_0\|=1.5\times(1.8028)=2.7042 \text{ sec}\\ T_2&=\mu\,\|\mathbf{P}_2-\mathbf{P}_1\|=1.5\times(2.8178)=4.2267 \text{ sec}\\ T_3&=\mu\,\|\mathbf{P}_3-\mathbf{P}_2\|=1.5\times(1.2806)=1.9209 \text{ sec}\\ T_4&=\mu\,\|\mathbf{P}_4-\mathbf{P}_3\|=1.5\times(1.5811)=2.3717 \text{ sec}\end{aligned}$$

The stop time is proposed as $\varepsilon = 1$ second. Therefore, each terminal-time $t_{f_i} = \sum_{j=1}^{i} T_j + i \times \varepsilon$ is given by

$$
\begin{aligned}
t_{f_1} &= T_1 + \varepsilon = 3.7042 \text{ sec} \\
t_{f_2} &= T_1 + T_2 + 2\varepsilon = 8.9309 \text{ sec} \\
t_{f_3} &= T_1 + T_2 + T_3 + 3\varepsilon = 11.8518 \text{ sec} \\
t_{f_4} &= T_1 + T_2 + T_3 + T_4 + 4\varepsilon = 15.2235 \text{ sec}
\end{aligned}
$$

For performing $K_i(t)$, $\dot{K}_i(t)$, $\ddot{K}_i(t)$, it is necessary to compute a_i, b_i, c_i as in (13), then it yields

$$a_1 = 0.05060;\ b_1 = 0.0561;\ c_1 = 0.0415 \tag{19a}$$
$$a_2 = 0.00132;\ b_2 = 0.0094;\ c_2 = 0.0044 \tag{19b}$$
$$a_3 = 0.14110;\ b_3 = 0.2203;\ c_3 = 0.2294 \tag{19c}$$
$$a_4 = 0.07500;\ b_4 = 0.0948;\ c_4 = 0.0800 \tag{19d}$$

Notice that with t_{f_i}, the activation functions can be computed, implying that (16), (17a) and (17a) can be performed with $n = 4$. In Fig. 3, the trajectory $\mathbf{l}_r(t)$ starting on $\mathbf{P}_0$ and steering through the points $\mathbf{P}_1$, $\mathbf{P}_2$, $\mathbf{P}_3$, $\mathbf{P}_4$ stooping on each one during a lapse of time $\varepsilon = 1$ second is depicted, by another hand the dynamical behavior of $\mathbf{l}_r(t)$ is observed in the following link: `https://youtu.be/li_jhjh75DE`. Even if, a naked eye, the trajectory can be appreciated as 'classical' one, the finite-time positioning properties is inner in it. These properties can be noted in Fig. 4, where their components x_{1r}(t) and $y_{1r}(t)$ are presented converging in finite time to the references x_{d_1}, x_{d_2}, x_{d_3}, x_{d_4} and y_{d_1}, y_{d_2}, y_{d_3}, y_{d_4} respectively. Note also that during a period time of $\varepsilon = 1$ second, the dynamics $x_{1r}(t)$ and $y_{1r}(t)$ hold over the mentioned references.

Therefore with the times T_i and t_{f_i} and with the previous coefficients a_i, b_i, c_i, the open loop controls $K_i(t)$, $\dot{K}_i(t)$, $\ddot{K}_i(t)$ are designed and also $\mathbf{l}_{\mathrm{P_{i-1}P_i}}(t)$, $\dot{\mathbf{l}}_{\mathrm{P_{i-1}P_i}}(t)$ and $\ddot{\mathbf{l}}_{\mathrm{P_{i-1}P_i}}(t)$ are eventually established. Now we can obtain the activation function $g_1(t)$, $f_1(t)g_2(t)$, $f_2(t)g_3(t)$, $f_3(t)g_4(t)$ and therefore obtain $\mathbf{l}_r(t)$, $\dot{\mathbf{l}}_r(t)$ and $\ddot{\mathbf{l}}_r(t)$ as

$$\mathbf{l}_r(t) = g_1(t)\mathbf{l}_{\mathrm{P_0P_1}}(t) + \sum_{i=2}^{4} f_{i-1}(t)g_i(t)\mathbf{l}_{\mathrm{P_{i-1}P_i}}(t) \tag{20a}$$
$$\dot{\mathbf{l}}_r(t) = g_1(t)\dot{\mathbf{l}}_{\mathrm{P_0P_1}}(t) + \sum_{i=2}^{4} f_{i-1}(t)g_i(t)\dot{\mathbf{l}}_{\mathrm{P_{i-1}P_i}}(t) \tag{20b}$$
$$\ddot{\mathbf{l}}_r(t) = g_1(t)\ddot{\mathbf{l}}_{\mathrm{P_0P_1}}(t) + \sum_{i=2}^{4} f_{i-1}(t)g_i(t)\ddot{\mathbf{l}}_{\mathrm{P_{i-1}P_i}}(t) \tag{20c}$$

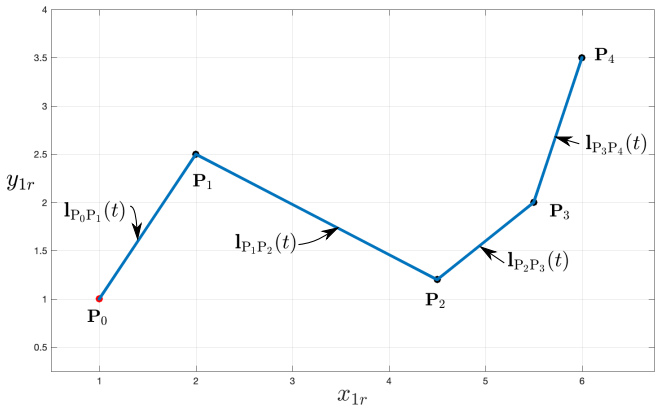

Fig. 3 Trajectory $\mathbf{l}_r(t) = (x_{1r}(t), y_{1r}(t))$ obtained from the five set-points

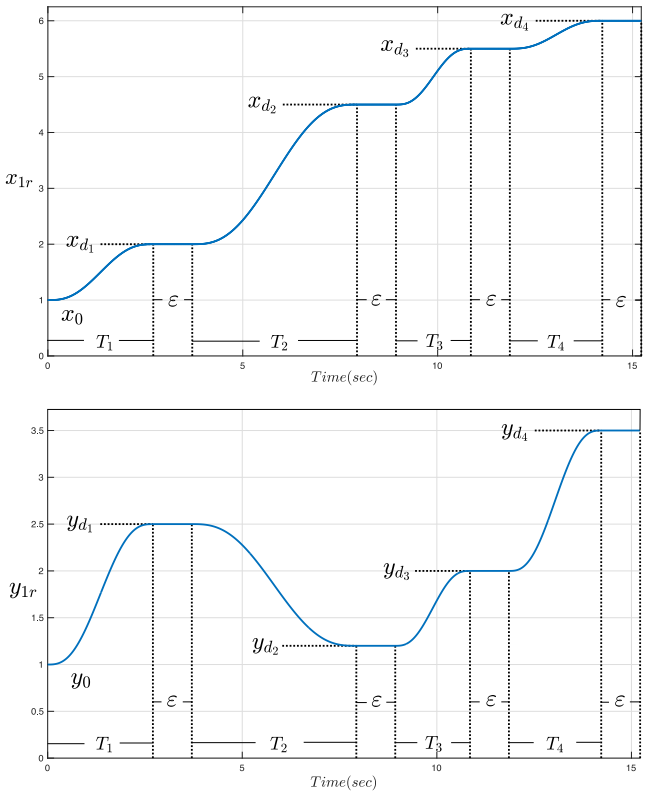

Fig. 4 Position x_{1r} and y_{1r} responses when the trajectory (16) is computed.

One of the main characteristics of the trajectory is to have zero velocity and acceleration at the beginning and ending of each part of the trajectory. These performances can be observed in Fig. 5 and Fig. 6. Note also that during the lapse of time of $\varepsilon = 1$ second these dynamics are holding on zero.

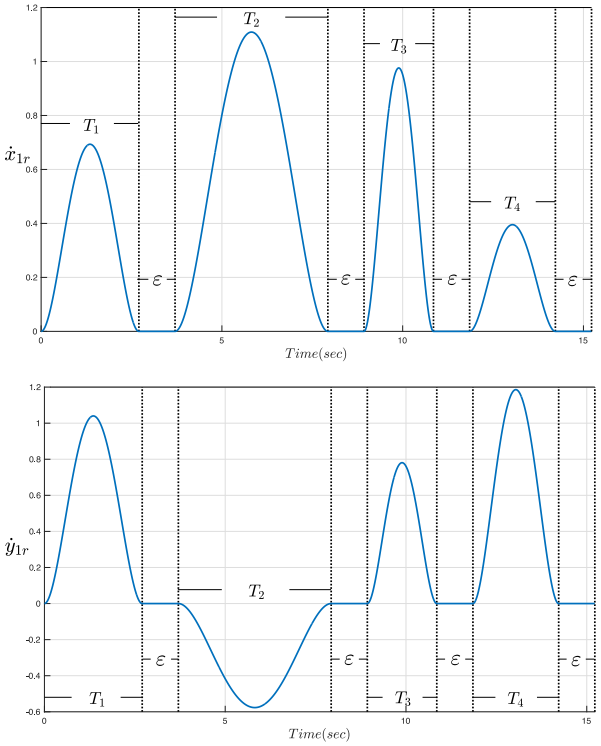

Fig. 5 Velocity dynamics $\dot{x}_{1r}$ and $\dot{y}_{1r}$ obtained when validating (17a)

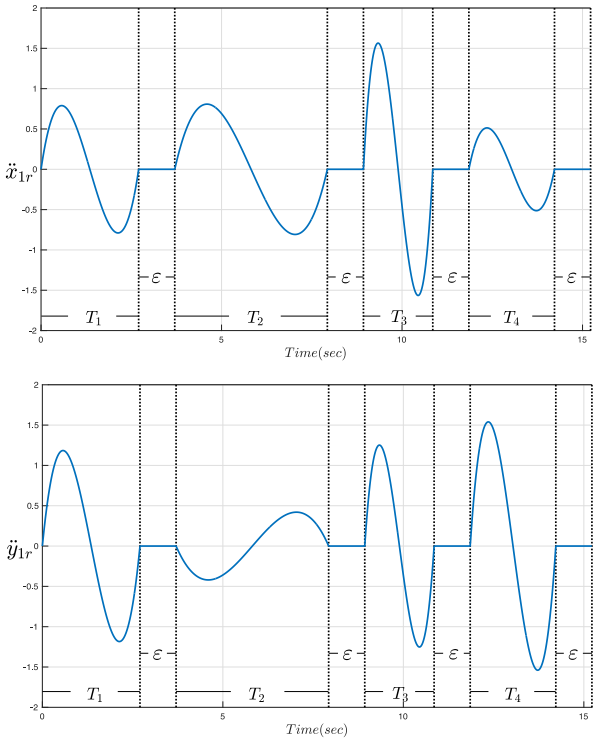

Fig. 6 Acceleration responses ($\ddot{x}_{1r}$, $\ddot{y}_{1r}$) of the trajectory composed by five points.

5 Simulation results

5.1 Control strategy for precision maneuvers: the cart example

The proposed trajectory with multiple finite time positioning can be used to conceive a control strategy for a robot that will let us to perform precision positioning maneuvers.

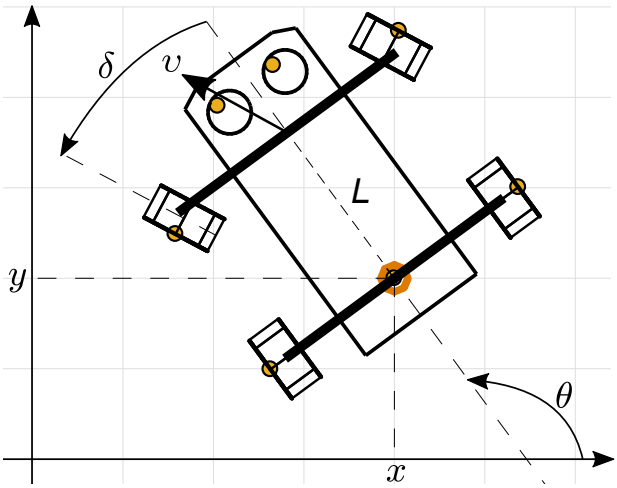

Fig. 7 Schematic representation of the cart.

In our case, the goal is to track with high precision trajectories using a ground robot. Therefore, firstly using Fig. 7, define its kinematic model as follows

$$\begin{cases} \dot{x} = \upsilon \cos(\delta)\cos(\theta) \\ \dot{y} = \upsilon \cos(\delta)\sin(\theta) \\ \dot{\theta} = \dfrac{\upsilon \sin(\delta)}{L} \end{cases} \tag{21}$$

where the car position is represented by the components x and y, the variable θ represents the orientation angle, and the control variables can be considered as

$\delta = u_1$: Steering angle control

$\upsilon = u_2$: Linear velocity control

Suppose that the ground vehicle in Figure 7 must be controlled to perform precision positioning maneuvers, passing for four sequential points $\mathbf{P}_0$, $\mathbf{P}_1$, $\mathbf{P}_2$, $\mathbf{P}_3$ that are distributed and aligned over the same straight line as can be seen in Fig. 8. These points (all in meters) are proposed as

$\mathbf{P}_0 = (x_0, y_0) = (1, 1.5)$: The initial position

$\mathbf{P}_1 = (x_{d_1}, y_{d_1}) = (1.32, 1.98)$

$\mathbf{P}_2 = (x_{d_2}, y_{d_2}) = (2.244, 3.366)$

$\mathbf{P}_3 = (x_{d_3}, y_{d_3}) = (2.6928, 4.0392)$

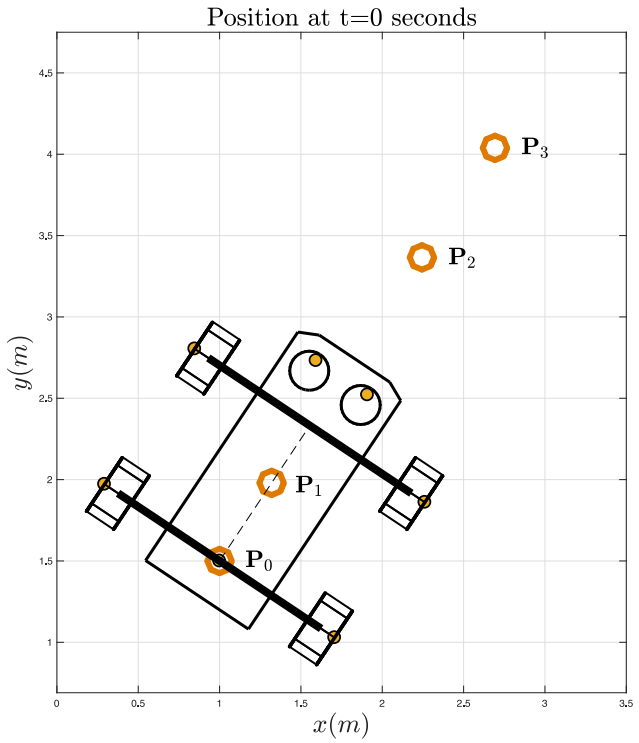

Fig. 8 Car in multiple finite time positioning.

Observed that for aligned points the orientation angle θ is constant, this means that $\theta(t) = \theta(0)$. This angle can be computed as $\theta = \arctan\left(\frac{y_{d_1} - y_0}{x_{d_1} - x_0}\right) = 0.9828$ radians $=$ 56.3099 degrees.

Being as, the orientation angle θ will remain invariant, obviously the steering control angle $(\delta = u_1)$ must be equal to zero once the angle is reached. Therefore, the linear velocity control $(\upsilon = u_2)$ is the only variable to control and accomplish that the car with initial position $\mathbf{P}_0$ moves autonomously over the sequential points $\mathbf{P}_1$, $\mathbf{P}_2$, $\mathbf{P}_3$. Likewise the car position (x, y) must be static over the above points during a lapse of time $\varepsilon = 0.5$ seconds.

From the above considerations (21) can be rewritten as

$$\begin{cases} \dot{x} = \upsilon \cos(\theta(0)) = \dot{x}_{1r} & x(0) = x_0 \\ \dot{y} = \upsilon \sin(\theta(0)) = \dot{y}_{1r} & y(0) = y_0 \\ \dot{\theta} = 0 & \theta(0) = 0.9828 \text{ rad} \end{cases} \tag{22}$$

Observe that $\dot{x}$ and $\dot{y}$ can be matched with $\dot{x}_{1r}$ and $\dot{y}_{1r}$ for computing υ. Therefore $\dot{x}^2 + \dot{y}^2 = \dot{x}_{1r}^2 + \dot{y}_{1r}^2 = \upsilon^2$, then

$$\upsilon = \sqrt{\left(\dot{x}_{1r}^2 + \dot{y}_{1r}^2\right)} \tag{23}$$

where $\dot{x}_{1r}$ and $\dot{y}_{1r}$ are given by

$$\dot{x}_{1r} = \dot{K}_1(t)\left(x_{d_1} - x_0\right) g_1(t) + \sum_{i=2}^{3} f_{i-1}(t) g_i(t) \dot{K}_i(t) \left(x_{d_i} - x_{d_{i-1}}\right)$$

$$\dot{y}_{1r} = \dot{K}_1(t)\left(y_{d_1} - y_0\right) g_1(t) + \sum_{i=2}^{3} f_{i-1}(t) g_i(t) \dot{K}_i(t) \left(y_{d_i} - y_{d_{i-1}}\right)$$

Therefore (23) becomes

$$\upsilon = \dot{K}_1(t) \|\mathbf{P}_1 - \mathbf{P}_0\| g_1(t) + \sum_{i=2}^{3} f_{i-1}(t) g_i(t) \dot{K}_i(t) \|\mathbf{P}_i - \mathbf{P}_{i-1}\|$$

Therefore the open loop velocity controls $\dot{K}_1(t)$, $\dot{K}_2(t)$, $\dot{K}_3(t)$ and the activation functions $g_1(t)$, $f_1(t)g_2(t)$, $f_2(t)g_3(t)$ are required to design $\dot{x}_{1r}$, $\dot{y}_{1r}$ and υ.

Firstly, the terminal times t_{f_i} and the convergence time T_i need to be computed as defined in Definitions 2 and 4.

For the convergence time T_i, a proportionality constant $\mu = 2.5$ is proposed, and according the right side from Table 1, it follows that

$$T_1 = \mu \|\mathbf{P}_1 - \mathbf{P}_0\| = 2.5 \times (0.5769) = 1.4422 \text{ seconds}$$
$$T_2 = \mu \|\mathbf{P}_2 - \mathbf{P}_1\| = 2.5 \times (1.6658) = 4.1644 \text{ seconds}$$
$$T_3 = \mu \|\mathbf{P}_3 - \mathbf{P}_2\| = 2.5 \times (0.8091) = 2.0227 \text{ seconds}$$

Then, the accumulative time t_{f_i} is determined by $t_{f_i} = \sum_{j=1}^{i} T_j + i \times \varepsilon$, thus,

$$t_{f_1} = T_1 + \varepsilon = 1.9422 \text{ seconds}$$
$$t_{f_2} = T_1 + T_2 + 2\varepsilon = 6.6066 \text{ seconds}$$
$$t_{f_3} = T_1 + T_2 + T_3 + 3\varepsilon = 9.1293 \text{ seconds}$$

From the previous, the activation time functions $g_1(t)$, $f_1(t)g_2(t)$ and $f_2(t)g_3(t)$ can be obtained. And from (13) a_i, b_i, c_i are given as

$$\mathrm{a}_1 = 0.3334;\ \mathrm{b}_1 = 0.6934;\ \mathrm{c}_1 = 0.9616 \tag{24a}$$
$$\mathrm{a}_2 = 0.0138;\ \mathrm{b}_2 = 0.0100;\ \mathrm{c}_2 = 0.0048 \tag{24b}$$
$$\mathrm{a}_3 = 0.1208;\ \mathrm{b}_3 = 0.1792;\ \mathrm{c}_3 = 0.1772 \tag{24c}$$

Fig. 9 shows the linear control velocity υ converging to zero in distinct finite times and during a lapse of time $\varepsilon = 0.5$ seconds the control velocity $\upsilon = 0$, corresponding when the vehicle is static.

In Fig. 10 the travelled distance represented by the variable S is illustrated. It is calculated as $S = \int_0^{t_{f_3}} \upsilon dt = \int_0^{t_{f_3}} \sqrt{\dot{x}_{1r}^2 + \dot{y}_{1r}^2} dt$.

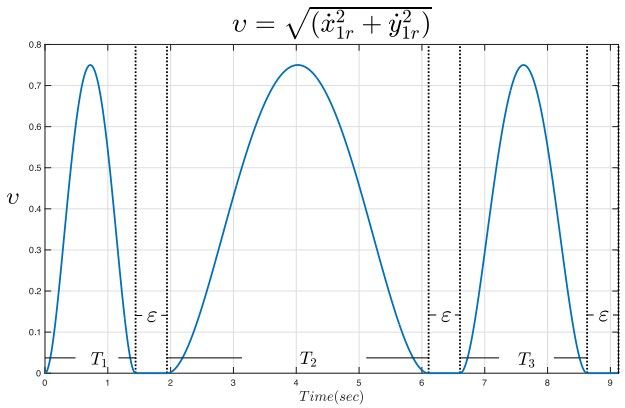

Fig. 9 Linear velocity control υ.

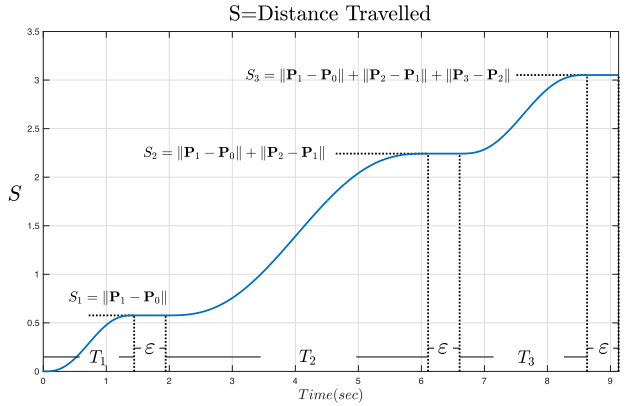

Fig. 10 Distance S versus the time t.

The distances S_1, S_2 and S_3 are all those that remain constants, corresponding when the car is not in motion during a lapse of time $\varepsilon = 0.5$ seconds, and S_3 is the total travelled distance.

In Fig. 11 the x and y states converge in finite time to the desired references x_{d_i} and y_{d_i}, respectively, and during the epsilon time $\varepsilon = 0.5$ seconds, the car is maintained static.

In a video animation, the car from the Fig. 8 moves over the points $\mathbf{P}_0$, $\mathbf{P}_1$, $\mathbf{P}_2$ and $\mathbf{P}_3$. The video can be viewed in the following link: `https://www.youtube.com/watch?v=5K37bXSNS5Q`.

5.2 Discussion results

In summary, the main advantage when applying the previous strategy is that the linear velocity υ is an open loop control guaranteeing the finite time convergence and therefore a state feedback control is not required. The previous implies that in real-time experiments the controllability can be achieved without measure the position in each moment.

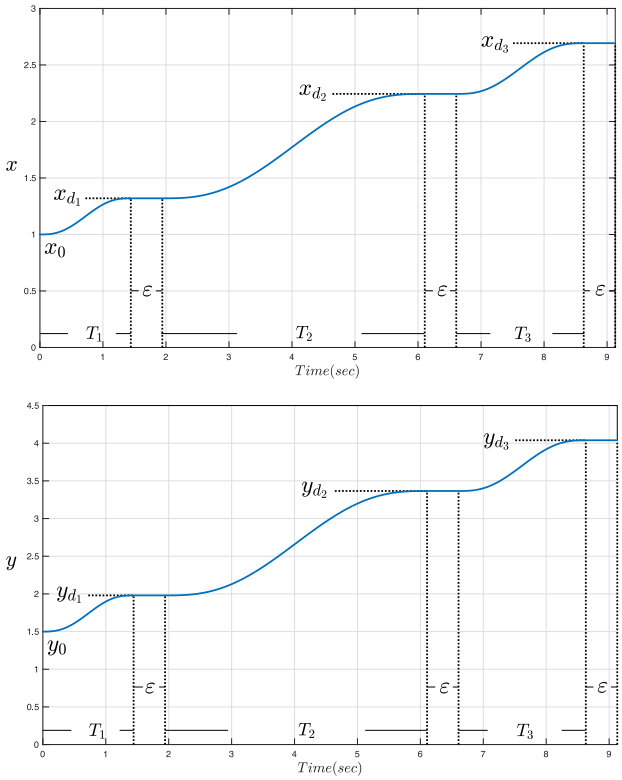

Fig. 11 Position dynamics x and y versus the time t.

6 Conclusions and future work

The proposed trajectory $\mathbf{l}_r(t)$ can be useful in route planning for mobile robots in applications that require higher precision. The control strategy was generated to design an *open loop control* of velocity υ for the kinematic car motion that allowed the finite time positioning over the statics points. In addition, the proposed theory can be useful in developing control strategies that guarantee the finite time convergence for a great diversity of aerial or ground mobile robots. Moreover, the above theory can be advantageous because we will not have the necessity to measure the position between the points $\mathbf{P}_{i-1}$ and $\mathbf{P}_i$. As consequence the sensors of position are not needed, implying a low cost if a real time implementation were required.

Conflict of Interest

The authors declare that we have not conflicts of interest regarding to the publication of this paper.

Data Availability

All data used to support the findings of this study are included within the article, and any additional support is available from the corresponding author upon request.

References

1. Brossard, M., Barrau, A., Bonnabel, S.: AI-IMU dead-reckoning. IEEE Transactions on Intelligent Vehicle, (2020)
2. Carreno, S., Wilson, P., Ridao, P., Petillot, Y.: A survey on terrain based navigation for AUVs. In: Oceans 2010 Mts/IEEE Seattle, pp. 1–7. IEEE (2010)
3. Filaretov, V., Zhirabok, A., Zyev, A., Protsenko, A., Tuphanov, I., Scherbatyuk, A.: Design and investigation of dead reckoning system with accommodation to sensors errors for autonomous underwater vehicle. In: OCEANS 2015-MTS/IEEE Washington, pp. 1–4. IEEE (2015)
4. Hossain, M.A., Kabir, K.A., Tanimoto, J.: Improved Car-Following Model Considering Modified Backward Optimal Velocity and Velocity Difference with Backward-Looking Effect. Journal of Applied Mathematics and Physics, **9**(2), 242–259, (2021)
5. Ilchmann, A., Ryan, E.P., Townsend, P.: Tracking control with prescribed transient behaviour for systems of known relative degree. Systems & Control Letters, **55**(5), 396–406, (2006)
6. Kao, W.W.: Integration of GPS and dead-reckoning navigation systems. In: Vehicle Navigation and Information Systems Conference, 1991, vol.2, pp. 635–643. IEEE (1991)
7. Levant, A., Alelishvili, L.: Transient adjustment of high-order sliding modes. In: Proc. of the 7th Scientific Workshop "Variable Structure Systems VSS, pp. 6–8. IEEE (2004)
8. Levant, A., Alelishvili, L.: Integral high-order sliding modes. IEEE Transactions on Automatic control, **52**(7), 1278–1282, (2007)
9. Li, Y., Zhang, L., Zheng, H., He, X., Peeta, S., Zheng, T., Li, Y.: Nonlane-Discipline-Based Car-Following Model for Electric Vehicles in Transportation- Cyber-Physical Systems. IEEE Transactions on Intelligent Transportation Systems, **19**(1), 38–47, (2018)
10. Mulvaney, D., Wang, Y., Sillitoe, I.: Waypoint-based mobile robot navigation. In: 2006 6th World Congress on Intelligent Control and Automation, **2**,9063–9067. IEEE (2006)
11. Nilles, A.Q., Becerra, I., LaValle, S.M.: Periodic trajectories of mobile robots. In: 2017 IEEE/RSJ International Conference on Intelligent Robots and Systems (IROS), pp. 3020–3026. IEEE (2017)
12. Oliveira, T., Peixoto, A., Nunes, E., Hsu, L.: Control of uncertain nonlinear systems with arbitrary relative degree and unknown control direction using sliding modes. International Journal of Adaptive Control and Signal Processing, **21**(8-9), 692–707, (2007)
13. Park, K., Chung, D., Chung, H., Lee, J.G.: Dead reckoning navigation of a mobile robot using an indirect Kalman filter. In: 1996 IEEE/SICE/RSJ International Conference on Multisensor Fusion and Integration for Intelligent Systems (Cat. No. 96TH8242), pp. 132–138. IEEE (1996)
14. Ramjattan, Allison N and Cross, Paul A.: A Kalman filter model for an integrated land vehicle navigation system. The Journal of Navigation, **48**(2), 293–302, (1995)
15. Reyes, S., Tokunaga, O.F., Espinoza, E.S., Salazar, S., Romero, H., Lozano, R.: Autonomous ground vehicle navigation using a novel visual positioning system. In: 2018 22nd International Conference on System Theory, Control and Computing (ICSTCC), pp. 342–347. IEEE (2018)
16. Sabet, M.T., Daniali, H.M., Fathi, A., Alizadeh, E.: Experimental analysis of a low-cost dead reckoning navigation system for a land vehicle using a robust AHRS, Robotics and Autonomous Systems, **95**, 37–51, (2017)
17. Shtessel, Y., Edwards, C., Fridman, L., Levant, A.: Sliding mode control and observation. Springer, (2014)
18. Wang, Y., Mulvaney, D., Sillitoe, I., Swere, E.: Robot navigation by waypoints. Journal of Intelligent and Robotic Systems, **52**(2), 175–207, (2008)
19. Welte, A., Xu, P., Bonnifait, P.: Four-wheeled dead-reckoning model calibration using rts smoothing. In: 2019 International Conference on Robotics and Automation (ICRA), pp. 312-318. IEEE (2019)
20. Yu, G., Wang, P., Wu, X., Wang, Y.: Linear and nonlinear stability analysis of a car-following model considering velocity difference of two adjacent lanes. Nonlinear Dynamics, **84**(1), 387–397, (2016)
21. Yu, S., Shi, Z.: Analysis of car-following behaviors considering the green signal countdown device. Nonlinear Dynamics, **82**(1), 731–740, (2015)
22. Zhang, L., Zhang, S., Zhou, B., Jiao, S., Huang, Y.: An Improved Car-Following Model considering Desired Safety Distance and Heterogeneity of Driver's Sensitivity. Journal of Advanced Transportation, **2021**, 12 pages, (2021)
23. Zheng, Z., Huo, W.: Navigation errors correction method based on magnetic nail positioning (2018). US Patent 9,864,379